

Journal of Materials Chemistry C

Accepted Manuscript



This article can be cited before page numbers have been issued, to do this please use: M. Cui, W. Li, L. Wang, L. Gong, H. Tang and D. Cao, *J. Mater. Chem. C*, 2019, DOI: 10.1039/C8TC05360J.



This is an Accepted Manuscript, which has been through the Royal Society of Chemistry peer review process and has been accepted for publication.

Accepted Manuscripts are published online shortly after acceptance, before technical editing, formatting and proof reading. Using this free service, authors can make their results available to the community, in citable form, before we publish the edited article. We will replace this Accepted Manuscript with the edited and formatted Advance Article as soon as it is available.

You can find more information about Accepted Manuscripts in the [author guidelines](#).

Please note that technical editing may introduce minor changes to the text and/or graphics, which may alter content. The journal's standard [Terms & Conditions](#) and the ethical guidelines, outlined in our [author and reviewer resource centre](#), still apply. In no event shall the Royal Society of Chemistry be held responsible for any errors or omissions in this Accepted Manuscript or any consequences arising from the use of any information it contains.

Twisted intramolecular charge transfer plus aggregation-enhanced emission active based quinoxaline luminogen: photophysical properties and a light-up fluorescent probe for glutathione

Mingming Cui,^{//} Wenting Li,^{//} Lingyun Wang,* Lingshan Gong, Hao Tang, Derong Cao

Key Laboratory of Functional Molecular Engineering of Guangdong Province, School of Chemistry and Chemical Engineering, South China University of Technology, Guangzhou, China, 510641

^{//}M.M. Cui and W.T. Li contributed equally.

*Corresponding author: Tel. +86 20 87110245; fax: +86 20 87110245. E-mail: lingyun@scut.edu.cn

Abstract

Developing solid and aggregate state emitters with large Stokes shift has long been a significant challenge in detection and bioimaging field. In this work, a novel quinoxaline-based luminogen (**QUPY**) with twisted intramolecular charge transfer (TICT) and aggregation-enhanced emission (AEE) characteristics has been designed and synthesized. Its pyridine salt derivative (**QUPY-S**) is also AEE-active and can be utilized as a fluorescent “turn-on” probe for the specific detection of GSH. The cleavage of dinitrophenyl ether of **QUPY-S** by GSH generated AEE-active and less water-soluble **QUPY**, which in turn opened “turn-on” fluorescence response around 516 nm. This reaction-based probe showed a large Stokes shift (131 nm), low detection limit (434 nM), fast response time, and low toxicity. **QUPY-S** was successfully applied to the detection of GSH in bovine serum samples with recoveries ranging from 91.9% to 100.7%. Additionally, **QUPY-S** can detect GSH in HeLa cells by confocal laser scanning micrographs.

Keywords: Aggregation-enhanced emission (AEE); GSH detection; Quinoxaline; Bioimaging

1 Introduction

As a “power house” to produce ATP, mitochondria participate in reactive oxygen species (ROS)-induced apoptosis. For instance, there are a large amount of free radical scavengers in mitochondria to protect cells from the oxidative stress. Intracellular thiols like glutathione (GSH), cysteine (Cys) and homocysteine (Hcy) can regulate the homeostasis of ROS through the respiratory chain of mitochondria [1-5]. As a critical antioxidant reservoir, mitochondrial GSH pool within cells plays important roles to keep oxidation-reduction equilibrium [6-7]. Moreover, abnormal levels of GSH may result in liver damage and neurogenic diseases and even cancer [8-12]. Therefore, it is urgent and important to develop a mitochondrial GSH probe for understanding mitochondrial associated diseases.

By taking advantage of the unique nucleophilicity of thiol group, discrimination of biothiols from other amino acids can be successfully achieved. However, identification of GSH from Cys/ Hcy was much more difficult due to bulkiness of GSH and its weak nucleophilicity [13-32]. Only very limited fluorescent probes targeted to detect GSH in mitochondria [33-40]. Unfortunately, most of reported sensors suffered from aggregation caused quenching (ACQ) effect and possessed small Stokes shifts. Especially, when they accumulated in cells, their fluorescence emission was much weaker than that in solutions and limited their use in vivo. Thus, it is of great interest to develop GSH probes with large Stokes shift and anti- ACQ effect for in vivo application.

Opposite to the photophysical phenomenon of ACQ, aggregation-induced emission (AIE) active fluorophores possessing strong fluorescence in their solid or aggregate

states attract more attentions. By manipulating aggregation/disaggregation process, various fluorescence turn-on probes based on AIE-active luminophores have been fabricated for sensitive detection of different analytes [41-42]. Moreover, because the nonplanar conformations of AIE molecules often lead to a loose packing in the solid state, linking a highly sterically bulky AIE moiety to a dye is expected to provide efficient solid-state emission. On the other hand, dyes with twisted intramolecular charge transfer (TICT) characteristics usually possess Stokes shifts larger than 100 nm [43-45]. In polar solvents, luminogens turn from the locally excited (LE) state at short wavelength to the TICT state at long wavelength through intramolecular rotation and result in large Stokes shift. During this process, charge separation between the donor and acceptor units occurs. Quinoxaline with tunable photophysical properties receives more attentions, because it is easy to construct donor and acceptor type structured luminogens through intramolecular charge transfer process [46-50].

Inspired by this design strategy, we covalently linked a popular AIE group (triphenylethylene) and pyridine moiety to quinoxaline core, resulting in a novel compound (**QUPY**) with AEE characteristics and large Stokes shifts through TICT process. Moreover, when the pyridinium group was functionalized by a dinitrophenoxy benzyl moiety to yield another AEE-active compound (**QUPY-S**), which can be utilized as a light-up probe for GSH detection. In the presence of GSH, the dinitrophenoxy benzyl group in **QUPY-S** was cleaved and regenerated **QUPY** with poor water solubility (Scheme 1). As a result, turn-on fluorescent probe for the specific detection of GSH was developed.

2 Experimental

2.1 Chemicals and instruments

Compound **1** and compound **3** were synthesized by previous reported methods, respectively [50, 39].

NMR spectra were recorded on Bruker advance III 400 MHz and chemical shifts were expressed in ppm using TMS as an internal standard. The UV-vis absorption spectra were recorded using a Helios Alpha UV-vis scanning spectrophotometer. Fluorescence spectra were obtained with a Hitachi F-4500 FL spectrophotometer with quartz cuvette (path length = 1 cm).

Absolute fluorescence quantum yield was measured by Hamamatsu spectrometer C11347, it consists of an excitation light source based on a xenon arc lamp and a high-sensitivity multichannel detector. The emitted light is collected by the integrating spheres. The use of integrating spheres has usually required a laser as the excitation source in combination with a fibre coupled CCD camera or a calibrated photodiode as the luminescence detectors.

The solutions of amino acids and anions were prepared from the corresponding nitrate salts or hydrochloride salts in deionized water. **QUPY-S** was dissolved in DMSO at room temperature to afford the stock solution (10^{-3} M). The PBS buffer were prepared with deionized water. The resulting solution was shaken well before recording the absorption and emission spectra.

3. Results and discussions

3.1 Design and synthesis of QUPY-S

The synthetic route to **QUPY-S** is shown in Scheme S1 (Supporting information). The palladium-catalyzed Suzuki coupling reaction of 5,8-dibromo-2,3-bis(4-methoxyphenyl)quinoxaline (compound **1**) and 1-boric acid ester -1,2,2-triphenylethylene afforded compound **2**. Further Suzuki coupling reaction of compound **2** with 4-pyridinylboronic acid produced compound **QUPY**. When treated **QUPY** in toluene under reflux with compound **3**, **QUPY-S** was obtained in 60% yield. The chemical structure of **QUPY-S** was confirmed by ^1H NMR, ^{13}C NMR and HRMS (Figures S1-S3, Supporting Information).

3.2 Photophysical properties of QUPY and QUPY-S

According to literatures ^[51], luminogens with a rotatable donor–acceptor (D-A) structure usually possess two excited states: a locally excited (LE) state and a TICT state. Meanwhile, increasing the polarity of the solvent can always bring the luminogens from the LE state to the TICT state, resulting in a large bathochromic shift in the emission wavelength and a dramatic decrease in the emission efficiency ^[52]. In our case, **QUPY** has D-A structure and AIE group (triphenylethylene). The photophysical properties of **QUPY** in DMSO–water mixtures were investigated with different water fractions, which is a combination of both strong AEE and TICT characteristics, as shown in Figure 1a. The locally-excited (LE) state at 473 nm is emissive in pure DMSO but its emission decreases as the solvent polarity is increased by adding water. At the 30% water fraction (f_w), the AEE state starts to dominate and

the emission is further enhanced. The emission wavelength of **QUPY** is bathochromically shifted from 473 to 519 nm during the solvent induced aggregation process due to the synergetic TICT-AEE effects. The fluorescence quantum yields of **QUPY** also increased from 4.3% in DMSO to 15.2% in DMSO/water (90:10, v/v). Meanwhile, distinct emission color changes from dark blue to bright green can be found. The aggregation of the **QUPY** in high water fraction was investigated by UV-vis spectrum and dynamic light scattering (DLS) measurements. As compared with **QUPY** in pure DMSO, the UV-vis spectrum of **QUPY** in 90% f_w was broader with level-off tails and baseline drifted, which in accordance of characteristics of nanoparticles due to Mie effect (Figure S4a). DLS measurements further indicated nanoparticles with 100 nm size were formed in presence of 90% f_w (Figure S4b).

In THF-water and CH₃CN-water mixtures, similar PL behaviors as that in DMSO-water mixtures were found (Figures 1b-1c). In addition, the remarkable 131 ~134 nm Stokes shift of **QUPY** was an advantage, facilitating its efficient signal in bioimaging and detection in living cells. In solid state, **QUPY** powder emitted bright green color (λ_{em} =517 nm) with 29.3% quantum efficiency (Figure 1d). Evidently, **QUPY** was both TICT and AEE characteristics.

As shown in Figure 2a, **QUPY-S** behaved differently. **QUPY-S** only showed a weak emission in DMSO (λ_{em} =566 nm) and almost had no change until f_w reached 40%. Afterward, the emission intensified swiftly. The emission intensity was boosted to the maximum when f_w was 70%, which was 15.5-fold higher than that in DMSO. With regard as fluorescence quantum yields, **QUPY-S** showed 10.4-fold enhancement from

2.6% in DMSO to 27.2% in DMSO/water (3/7, v/v). When f_w was beyond 70%, the emission intensity began to decrease. It is possible that the molecules might agglomerate quickly to form small and tight aggregates in presence of high f_w , which was verified by DLS data for 705 nm and 243 nm in presence of 70% and 90% f_w , respectively (Figures S5a,5b). The decrease in the emission intensity of QUPY-S when the water fraction is increased from 70% to 90% may be attributed to the change in the packing mode of the molecules in the aggregates. In the mixture with the “low” water content, the molecules may steadily assemble in an ordered fashion to form more emissive crystalline aggregates. At water fractions above 70%, the molecules may quickly agglomerate in a random way to form less emissive amorphous particles with small size. Similar results have been reported by others [53].

In addition, the emission of QUPY-S in DMSO/ glycerol mixture with various viscosity was carried out (Figure 2b). The highest fluorescence intensity was observed in 90% glycerol fraction, where 9.3-fold emission enhancement was present than that in DMSO. Moreover, the fluorescence spectrum of QUPY-S in the solid state were recorded and shown in Figure 2c, where emission peak at 584 nm with 18.9% quantum efficiency was present. Thus, QUPY-S feature the unique AEE characteristics.

3.3 Spectral Properties of QUPY-S with GSH

To demonstrate that QUPY-S can be used as a light-up probe, we measured fluorescence response of QUPY-S in H₂O/DMSO (1:1, v/v) after incubation with 10 equiv. GSH at 37 °C for 90 min (Figure 3). Before incubating with GSH, QUPY-S was

weakly emissive at 566 nm. However, the emission at 516 nm emerged after incubation with GSH. The fluorescence intensity at 516 nm increased by 12.5 times when the concentration of GSH reached 100 μM . Meanwhile, such fluorescence enhancement can be distinguished with naked-eye as shown in the inset of Figure 3, where the color changed from dark orange to bright green before and after incubation with GSH under UV light illumination. This experiment showed that **QUPY-S** was potential to be used as a fluorescent light-up probe.

The quantitative determinations were measured with **QUPY-S** by incremental addition of GSH and the turn-on response at 516 nm was measured. As shown in Figure 4a, it can be seen that the fluorescence intensity of the **QUPY-S** gradually increases upon gradual increase of GSH level. Moreover, a good linear relationship with R^2 of 0.996 between the fluorescent intensity at 516 nm in the range of 0 to 10 μM can be found (Figure 4b). The limits of detection (LOD) were determined from the equation $\text{LOD} = 3\sigma/K$, where σ is the standard deviation of the blank solution and K is the slope of the calibration curve. The limits detection of **QUPY-S** was determined to be 434 nM for GSH detection, which was at the nearly same level with other results (Table S1).

3.4 Selectivity and pH effect of **QUPY-S** for detecting GSH

Since GSH is the most predominant biological thiol in cells and mimicking typical concentration in blood, GSH (1 mM), Cys (80 μM), Hcy (80 μM) and NaSH (50 μM) were used to evaluate the selectivity **QUPY-S**. Figure 5a showed time-dependent of fluorescence intensity at 516 nm of **QUPY-S** in DMSO/PBS buffer (1:1, v/v, pH 7.4)

at 37 °C in presence of these analytes. GSH induced 12.1-fold fluorescence enhancement while Cys, Hcy and NaSH only showed no more than 2.1-fold enhancement within 30 min. If we shortened incubation time to 9 min, selectivity of **QUPY-S** for GSH detection was improved, where GSH intensified 8.3-fold emission strength while others caused slight fluorescent enhancement (Figure 5b). In addition, different kinds of amino acids (Ala, Asp, Glu, Gly, Asr, Leu, Lys, Met, Phe, Ser, Thr, Trp, Tyr, Val), some physiological related neurochemical transition metal ions (Fe^{3+} , Cu^{2+} , Mn^{2+} , Zn^{2+}), reactive nitrogen species NO_2^- , reactive sulfur species (HSO_3^- , SO_3^{2-} , $\text{S}_2\text{O}_5^{2-}$), anions and other possible interferences were chosen to measure the spectral response. As shown in Figure S6-S7, no obvious fluorescence response was displayed, which confirmed that **QUPY-S** exhibited high selectivity for detecting GSH.

As shown in Figure S8, the reaction capacity of **QUPY-S** to GSH was pH-dependent. The higher fluorescence “Turn On” observation along with increased pH value can be found. This can be explained by higher concentration of thiolate species in high pH environment. In this work, pH of 7.4 with DMSO/PBS buffer (1/1) was selected as the standard sensing conditions.

3.5 Mechanism of GSH Sensing

As we know, dinitrophenyl nitro group can be utilized as the GSH-selective reaction unit [54-58]. The fluorescence enhancement observed for **QUPY-S** in presence of GSH can be attributed to the transformation of **QUPY-S** into AEE-active **QUPY**, which easily aggregated in detection solution, leading to fluorescence enhancement. This

assumption was supported by the following results: (i) the absorption and fluorescence spectra of **QUPY-S** after incubation with GSH overlaps well with that of **QUPY** in the same solution (Figure S9); (ii) the mass signal at $m/z = 674.419$, corresponding to the molecular weight of $[\text{QUPY} + \text{H}]^+$, was found after the reaction solution of **QUPY-S** and GSH (Figure S10). According to Scheme S2, compound **5** originated from active quinone-methide species attacked by GSH as well as compound **4** would generate simultaneously. In fact, two signals at $m/z = 399.1058, 496.1762$ corresponding to the molecular weight of $[\text{5} + \text{H}]^+, [\text{4} + \text{Na}]^+$ were observed, respectively (Figure S11). As displayed in Figure S12, **QUPY-S** in DMSO/PBS buffer (v/v, 1/1) formed aggregates of ca. 106.4 nm and possessed +93.9 mV Zeta potential. After incubation with GSH (100.0 μM), larger aggregates of ca. 251.2 nm were present, supporting the transformation of **QUPY-S** into more hydrophobic **QUPY** after reaction with GSH (Figure S12). At the same time, Zeta potential was also reduced to +34.6 mV.

Compared with Cys and Hcy, GSH has highest pK_a , largest steric bulkiness and lowest reactivity, why did **QUPY-S** show highest reactivity to GSH? The proposed pyridinium modulated S_NAr reaction mechanism for selective recognition of GSH was illustrated in Scheme S2. Some possibilities can be included: (1) the steric fit of the carboxylate group in three biothiols is optimal in GSH, and (2) the pyridinium cation in **QUPY-S** may have the strongest electrostatic interaction with carboxylate group in GSH, thus might modulate the S_NAr attack of the thiol group in GSH against dinitrophenoxy moiety. Such electrostatic interaction may accelerate the reaction rate of GSH for S_NAr attack significantly. In contrast, Cys and Hcy are not affected much.

Since Cys and Hcy are shorter than GSH (HS- carboxylate separation: 3 bonds for Cys, 4 bonds for Hcy, 8 bonds for GSH), they cannot generate strong electrostatic interaction with cationic pyridinium and thiol groups in Cys and Hcy failed to reach the reactive site of dinitrophenoxy moiety. Some similar selective GSH fluorescent probes have been reported ^[59].

3.6 The Density Functional Theory Investigations

The theoretical calculations with a B3LYP/6-31G (d) basis set was performed to gain more insight into molecular orbital and charge distribution of **QUPY-S** and **QUPY**. As shown in Figure S13, the electrons on the HOMO and LUMO of **QUPY-S** were distributed on the two marginal sides of triphenylethene groups and dinitrophenoxy benzyl pyridinium moiety, respectively. This might cause the possible photoinduced electron transfer (PET) process in **QUPY-S** and weak fluorescence. However, the electron densities of the HOMO of **QUPY** was mainly located on the quinoxaline core and triphenylethene units, LUMO is mostly localized on the central quinoxaline core and pyridine ring, which indicated that there was partial electronic conjugation between them. In presence of GSH, **QUPY-S** converted to **QUPY** by removal dinitrophenoxy benzyl moiety and the energy gap (E_g) value also increased from 2.54 eV to 3.40 eV, which was in good accordance with the fluorescence “turn on” response.

3.7 Detection applications in Complex Biological Samples

The practical application of **QUPY-S** was examined by quantitative determining

GSH fluorometrically in complicated biological samples - bovine serum albumin (BSA). When serum sample was added into **QUPY-S** (10 μM), the emission intensity at 516 nm was enhanced. On the basis of the linear relationship of between the fluorescence intensity at 516 nm and concentration of GSH in Figure 4b, the concentration of GSH in the bovine serum albumin (BSA) sample was determined to be 1.67 μM . In order to confirm the observed emission enhancement at 516 nm was due to presence of GSH, a known concentration of GSH was added into the same solution. It can be found more intense emission peak at 516 nm was present. As shown in Table S2, the recovery of the spiked samples ranged between 91.9% and 100.7%, indicating the practicability of the proposed sensing platform. These results confirmed presence of GSH in blood serum sample, thus resulting in fluorescence enhancement. So, **QUPY-S** can be used for the determination of GSH in real samples.

3.8 Bioimaging of probe **QUPY-S** in living cells

The photostability of **QUPY-S** in DMSO/PBS buffer (v/v, 1/1) under continuous 365 nm irradiation was investigated. With increasing irradiation time, the maximal absorbance of the **QUPY-S** at 411 nm showed only a negligible decrease of absorbance (Figure S14). These results indicated that **QUPY-S** had good photostability.

Biocompatibility is important to be taken into account in an intracellular probe for bioimaging. As shown Figure S15, **QUPY-S** showed *in vitro* low toxicity toward cultured HeLa cell lines under the experimental conditions through the CCK-8 assay. Similarly, **QUPY** showed no apparent toxicity to the cells. So, **QUPY-S** and **QUPY**

were favorable for imaging in living cells due to excellent biocompatibility.

View Article Online
DOI: 10.1039/C8TC05360J

Confocal microscopy experiments were carried out to bioimage and monitor of GSH in living cells with **QUPY-S**. As shown in Figure 6a, when HeLa cells were incubated with **QUPY-S** (0.05 mM), strong yellow fluorescence was observed inside the cells, which can be ascribed to the presence of endogenous GSH reacting with **QUPY-S**. However, if HeLa cells were pre-treated with excess N-ethylmaleimide (NEM), a trapping reagent for thiol species, followed by treatment with **QUPY-S** (0.5 mM), only a negligible fluorescence signal was present (Figure 6c). The further addition of 200 mM of an exogenous GSH also led to an obvious fluorescence enhancement (Figure 6e). These results demonstrating the ability of **QUPY-S** to detect GSH in HeLa cells. The yellow-fluorescence image in HeLa cells is further supported by Lambda mode of confocal microscope and corresponding spectrum (Figures S16-S17), which can be ascribed to interactions between **QUPY** and multiple factors such as weak acidity, protein, ions and complex physiological environment of cells.

4 Conclusions

A triphenylethylene-containing quinoxaline pyridinium compound (**QUPY**) and its salt (**QUPY-S**) were synthesized and investigated. **QUPY** showed both TICT and AEE characteristics with large Stoke shifts. **QUPY-S** was also AEE-active. As a new selective fluorescence turn-on detection of GSH, **QUPY-S** can be transformed into **QUPY** by removal of 2,4-dinitrophenyl group in presence of GSH in aqueous solution, and the subsequent aggregation of **QUPY** turns on the emission with the detection limit

of 434 nM. The electrostatic interaction to modulate the attack of GSH is believed to play significant role for high selectivity. **QUPY-S** has been successfully used to detect in complex biological samples and mitochondrial GSH in HeLa cells.

Acknowledgements

The supports by the Natural Science Foundation of Guangdong Province (2015A030313209, 2016A030311034) and the Fundamental Research Funds for the Central Universities (2017ZD075) are gratefully acknowledged.

References

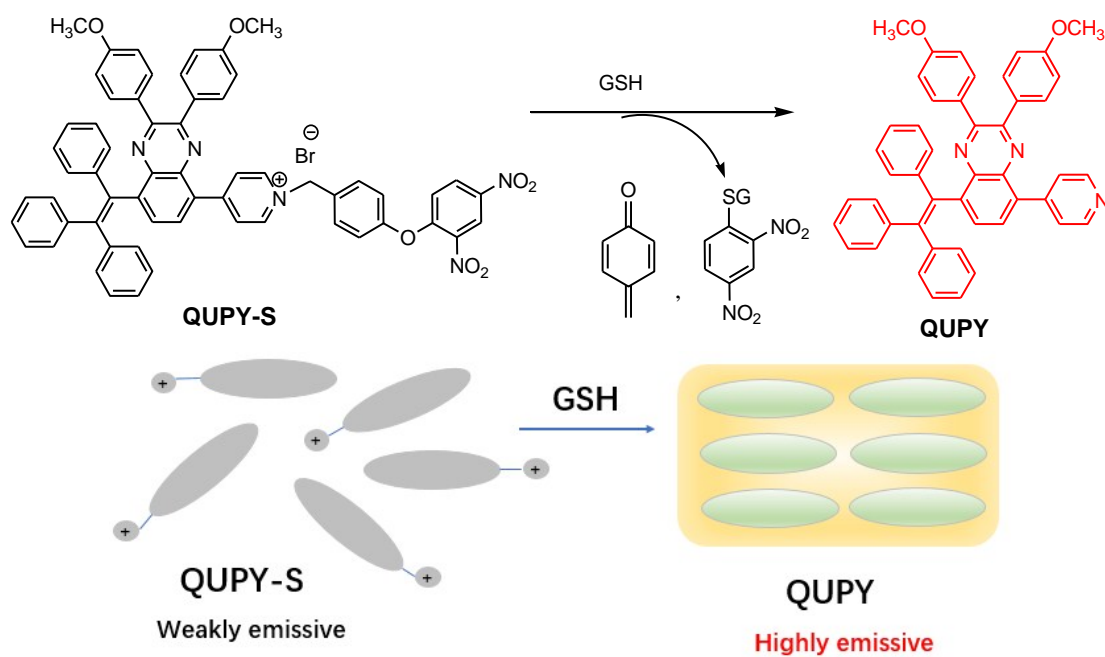
- [1] R. S. Balaban, S. Nemoto, T. Finkel, *Cell*, 2005, **120**, 483–495.
- [2] M. Schwarzländer, I. Finkemeier, *Antioxid. Redox Signal*, 2013, **18**, 2122–2144.
- [3] Z. A. Wood, E. Schroder, J. Robin Harris, L. B. Poole, *Trends Biochem. Sci.*, 2003, **28**, 32–40.
- [4] B. Morgan, D. Ezerin, T. N. Amoako, J. Riemer, M. Seedorf, T. P. Dick, *Nat. Chem. Biol.*, 2013, **9**, 119–125.
- [5] S. Shahrokhian, *Anal. Chem.*, 2001, **73**, 5972–5978.
- [6] H. Tapiero, D. Townsend, K. Tew, *Biomed. Pharmacother.*, 2003, **57**, 134–144.
- [7] H. S. Jung, J. H. Han, T. Pradhan, S. Kim, S. W. Lee, J. L. Sessler, T. W. Kim, C. Kang, J. S. Kim, *Biomaterials*, 2012, **33**, 945–953.
- [8] S. Seshadri, A. Beiser, J. Selhub, P. F. Jacques, I. H. Rosenberg, R. B. D'Agostino, P. W. Wilson, P. A. Wolf, *New Engl. J. Med.*, 2002, **346**, 476–483.
- [9] Y. X. Guo, X. F. Yang, L. Hakuna, A. Barve, J. O. Escobedo, M. Lowry, M. Strongin, *Sensors*, 2012, **12**, 5940–5950.
- [10] J. J. He, F. Y. Yan, D. P. Kong, Q. H. Ye, X. G. Zhou, L. Chen, *Curr. Org. Chem.* 2016, **20**, 2718–2734.
- [11] A. Wahlländer, S. Soboll, H. Sies, I. Linke, M. Müller, *Febs. Lett.*, 1979, **97**, 138–140.
- [12] P. C. Jocelyn, *Biochim. Biophys. Acta*, 1975, **396**, 427–436.
- [13] P. Wang, J. Liu X. Lv, Y. Liu, Y. Zhao, W. Guo, *Org. Lett.*, 2012, **14**, 520–531.
- [14] C. J. Wang, X. Xia, J. Luo, Q. Wang, *Dyes. Pigm.*, 2018, **152**, 85–92.

- [15] K. Balasubramanian, H. Swaminathan, *Sensor. Actuat. B-Chem.*, 2018, **259**, 980–989.
- [16] O. Y. Juan, C. Y. Li, Y. Li, J. Fei, F. Xu, J. Li, X. Nie, *Sensor. Actuat. B-Chem.*, 2017, **240**, 1165–1173.
- [17] X. Jiang, F. Geng, Y. Wang, J. H. Liu, P. Qu, M. Xu, *Biosens. Bioelectron.*, 2016, **81**, 268–273.
- [18] H. Zhang, C. Wang, Ge. Wang, K. Wang, K. Jiang, *Biosens. Bioelectron.*, 2016, **78**, 344–350.
- [19] L. Pang, Y. Zhou, E. Wang, F. Yu, H. Zhou, W. L. Gao, *Rsc. Adv.* 2016, **6**, 16467–16473.
- [20] C. Xu, H. Li, B. Yin, *Biosens. Bioelectron.*, 2015, **72**, 275–281.
- [21] Z. Guo, S. Nam, S. J. Park, *Chem. Sci.*, 2012, **3**, 2760–2772.
- [22] X. Yang, Y. Guo, R.M. Strongin, *Angew. Chem., Int. Ed.*, 2011, **50**, 10690–10696.
- [23] W. Wang, O. Rusin, X. Xu, O. Jorge, A. Kristin, M. Fletcher, M. Corin, C. Schowalter, F. Lawrence, I. Fronczek, M. Robert, *J. Am. Chem. Soc.*, 2005, **127**, 15949–15952.
- [24] O. Rusin, K. Lian, R. M. Strongin, *J. Am. Chem. Soc.*, 2004, **126**, 438–439.
- [25] F. Wang, L. Zhou, C. Zhao, R. Wang, Q. Fei, S. Luo, Z. Guo, W. H. Zhu, *Chem. Sci.*, 2015, **6**, 2584–2589.
- [26] X. F. Yang, Q. Huang, Y. Zhong, L. Zheng, Hua. Li, J. Escobedoc, R. M. Strongin, *Chem. Sci.*, 2014, **5**, 2177–2183.
- [27] M. Isik, R. Guliyev, E. U. Akkaya, *Org. Lett.*, 2014, **16**, 3260–3263.

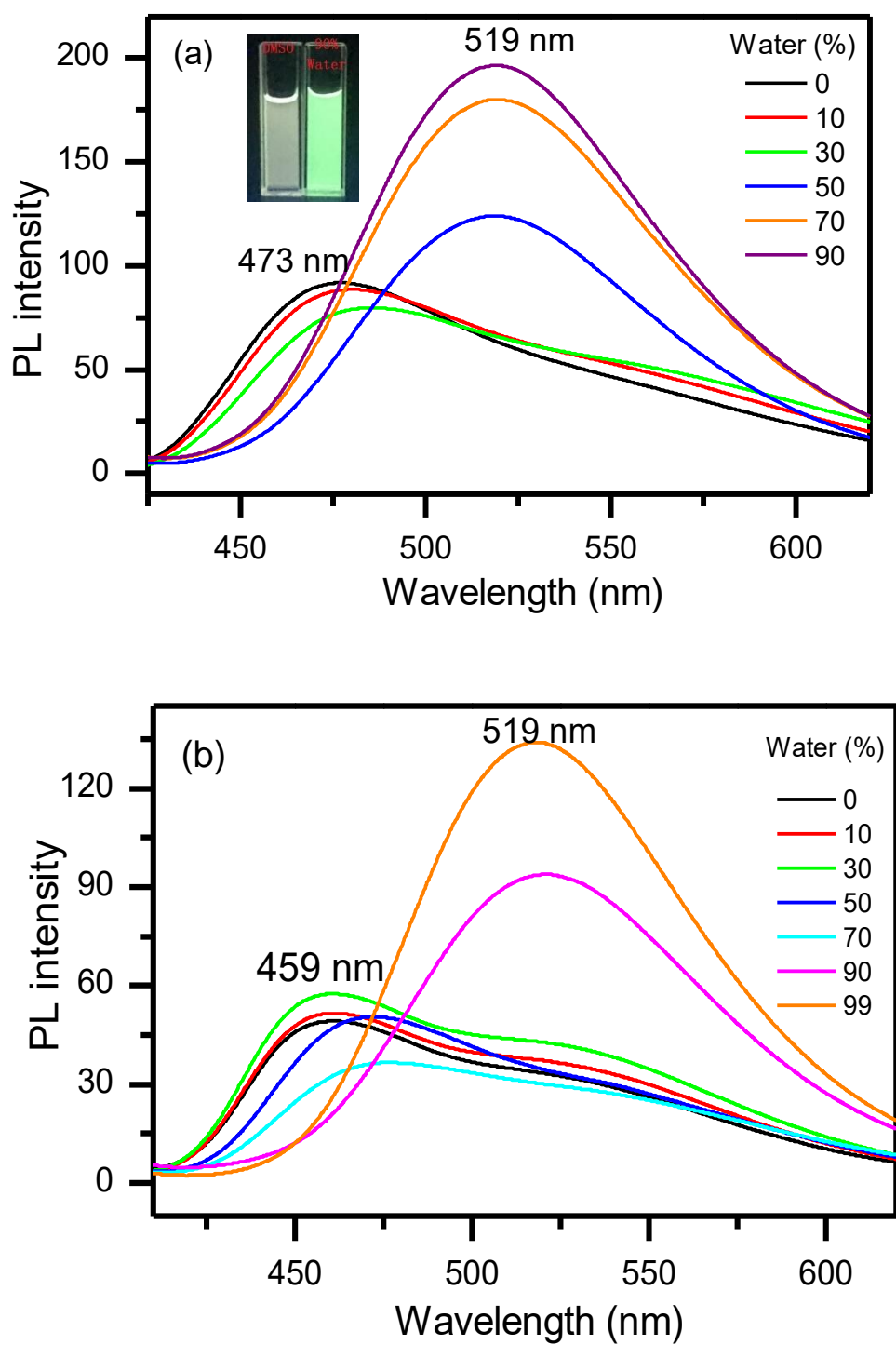
- [28] L. Niu, Y. Guan, Y. Chen, L. Wu, C. Tung, Q. Z. Yang, *J. Am. Chem. Soc.*, 2012, **134**, 18928–18931. View Article Online
DOI: 10.1039/C8TC05360J
- [29] J. Yin, Y. Kwon, D. Kim, D. Lee, G. Kim, Y. Hu, J. Yoon, *J. Am. Chem. Soc.*, 2014, **136**, 5351–5358.
- [30] S. A. Zaidi, J. H. Shin, *Anal. Methods*, 2016, **8**, 1745–1754.
- [31] H. Chen, Y. Tang, W. Lin, *Trends Anal. Chem.*, 2016, **76**, 166–188.
- [32] S. Lee, J. Li, X. Zhou, J. Yin, J. Yoon, *Coord. Chem. Rev.*, 2018, **366**, 29–68.
- [33] C. Lim, G. Masanta, H. Kim, J. Han, H. Kim, B. Cho, *J. Am. Chem. Soc.*, 2011, **133**, 11132–11135.
- [34] S. Lim, K. Hong, D. Kim, H. Kwon, H. Kim, *J. Am. Chem. Soc.*, 2014, **136**, 7018–7025.
- [35] Niu, L.-Y. Chen, Y.-Z. Zheng, H.-R. Wu, L.-Z. Tung, C.-H. Yang, Q.-Z. *Chem. Soc. Rev.*, 2015, **44**, 6143–6160.
- [36] X. L. Liu, L. Y. Niu, Y. Z. Chen, Y. X. Yang, Q. Z. Yang, *Biosens. Bioelectron.*, 2017, **90**, 403–409.
- [37] X. L. Liu, L. Y. Niu, Y. Z. Chen, M. L. Zheng, Y. Yang, Q. Z. Yang, *Org. Biomol. Chem.*, 2017, **15**, 1072–1075.
- [38] M. Y. Jia, L. Y. Niu, Y. Zhang, Q. Z. Yang, C. Tung, Y. F. Guan, L. Feng, *ACS Appl. Mater. & Interfaces*, 2015, **7**, 5907–5914.
- [39] J. Zhang, X. Bao, J. Zhou, F. Peng, H. Ren, X. Dong, W. Zhao, *Biosens. Bioelectron.*, 2016, **85**, 164–170.
- [40] C. Zhan, G. Zhang, D. Zhang, *ACS Appl. Mater. Interfaces*, 2018, **10**, 12141–12149.

- [41] F. Biedermann, E. Elmalem, I. Ghosh, W. M. Nau, O. A. Scherman, *Angew. Chem. Int. Ed.*, 2012, **51**, 7739–7743.
- [42] J. Mei, N. Leung, R. Kwok, J. W. Y. Lam, B. Z. Tang, *Chem. Rev.*, 2015, **115**, 11718–11940.
- [43] R. Hu, E. Lager, A. Aguilar, J. Liu, Y. Zhong, K. S. Wong, B. Z. Tang, *J. Phys. Chem. C*, 2009, **113**, 15845–15851.
- [44] R. Hu, W. Y. Lam, S. Chen, R. Ye, Y. Zhong, B. Z. Tang, *Chem. Commun.*, 2012, **48**, 10099–10101.
- [45] C. F. A. Gomez-Duran, R. Hu, G. Feng, T. Li, F. Bu, B. Z. Tang, *ACS Appl. Mater. Interfaces*, 2015, **7**, 15168–15176.
- [46] Z. F. Chang, L. M. Jing, B. Chen, M. Zhang, X. Cai, J. J. Liu, Y. C. Ye, B. Liu, J. L. Wang, B. Z. Tang, *Chem Sci.*, 2016, **7**, 4527–4536.
- [47] Z. F. Chang, L. M. Jing, C. Wei, Y. P. Dong, Y. C. Ye, Y. S. Zhao, J. L. Wang, *Chem Eur J.*, 2015, **21**, 8504–8510.
- [48] A. Ekbote, T. Jadhav, R. Misra, *New J Chem.*, 2017, **41**, 9346–9353.
- [49] Y. Chen, Y. Ling, L. Ding, C. Xiang, G. Zhou, *J. Mater. Chem. C*, 2016, **4**, 8496–8505.
- [50] L. Wang, M. Cui, H. Tang, D. Cao. *Dyes. Pigm.*, 2015, **155**, 107–113.
- [51] (a) A. Ito, S. Ishizaka and N. Kitamura, *Phys. Chem. Chem. Phys.*, 2010, **12**, 6641–6649. (b) P. Mahato, S. Saha and A. Das, *J. Phys. Chem. C*, 2012, **116**, 17448–17457.
- [52] (a) T. Han, W. Wei, J. Yuan, Y. Duan, Y. Li, L. Hu and Y. Dong, *Talanta*, 2016, **150**, 104–112. (b) A. Nicol, W. Qin, R. T. Kwok, J. M. Burkhartsmeier, Z. Zhu, H. Su, W.

- Luo, J. W. Lam, J. Qian and K. S. Wong, *Chem. Sci.*, 2017, **8**, 4634–4643. View Article Online
DOI: 10.1039/C8TC05360J
- [53] (a) Y. Dong, J. W. Y. Lam, A. Qin, J. Sun, J. Liu, Z. Li, J. Sun, H. H. Y. Sung, I. D. Williams, H. S. Kwok and B. Z. Tang, *Chem. Commun.*, 2007, 3255–3257. (b) X. Zheng, Q. Peng, L. Zhu, Y. Xie, X. Huang and Z. Shuai, *Nanoscale*, 2016, **8**, 15173–15180.
- [54] S. Gnaim, D. Shabat, *Acc. Chem. Res.*, 2014, **47**, 2970–2984.
- [55] H. Xiao, K. Xin, H. Dou, G. Yin, Y. Quana, R. Wang, *Chem. Commun.*, 2015, **51**, 1442–1445.
- [56] J. Xu, Q. Li, Y. Yue, Y. Guo, S. Shao, *Biosens. Bioelectron.*, 2014, **56**, 58–63.
- [57] P. Yue, X. Yang, P. Ning, X. Xi, H. Yu, Y. Feng, R. Shao, X. Meng, *Talanta*, **2018**, 178, 24–30.
- [58] Y. Li, K. Wang, M. Li, N. Zong, W. Mao, *Sensor Actuat B-chem.*, 2018, **255**, 193–202.
- [59] (a) J. Yin, Y. Kwon, D. Kim, D. Lee, G. Kim, Y. Hu, J.-H. Ryu and J. Yoon, *J. Am. Chem. Soc.*, 2014, **136**, 5351–5358. (b) M. Isık, R. Guliyev, S. Kolemen, Y. Altay, B. Senturk, T. Tekinay and E. U. Akkaya, *Org. Lett.*, 2014, **16**, 3260–3263. (c) J. Zhang, X. Bao, J. Zhou, F. Peng, H. Ren, X. Dong, W. Zhao, *Biosensors Bioelectronics*, 2016, **85**, 164–170.



Scheme 1 Schematic representation of light-up sensing of GSH by QUPY-S.



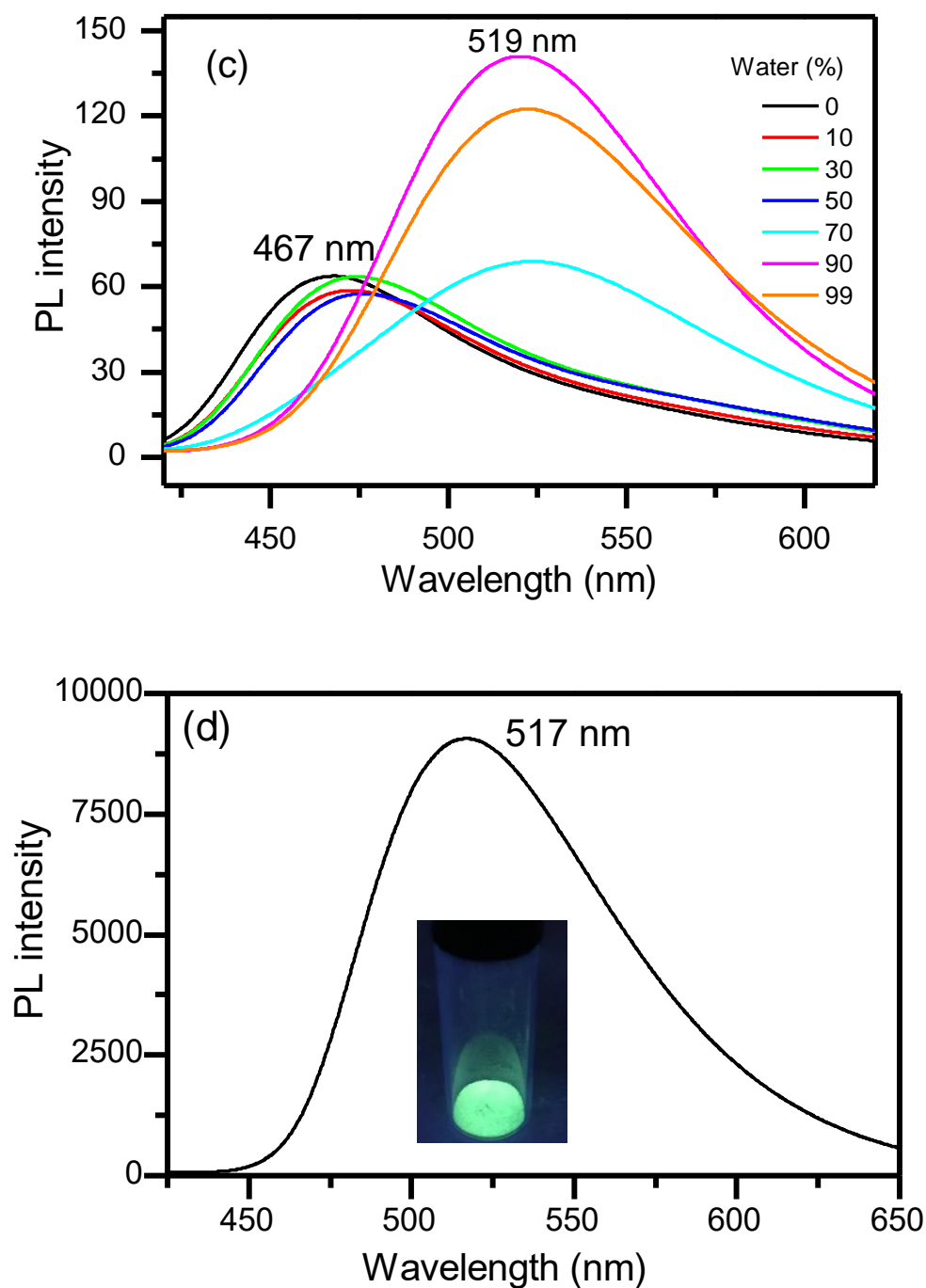
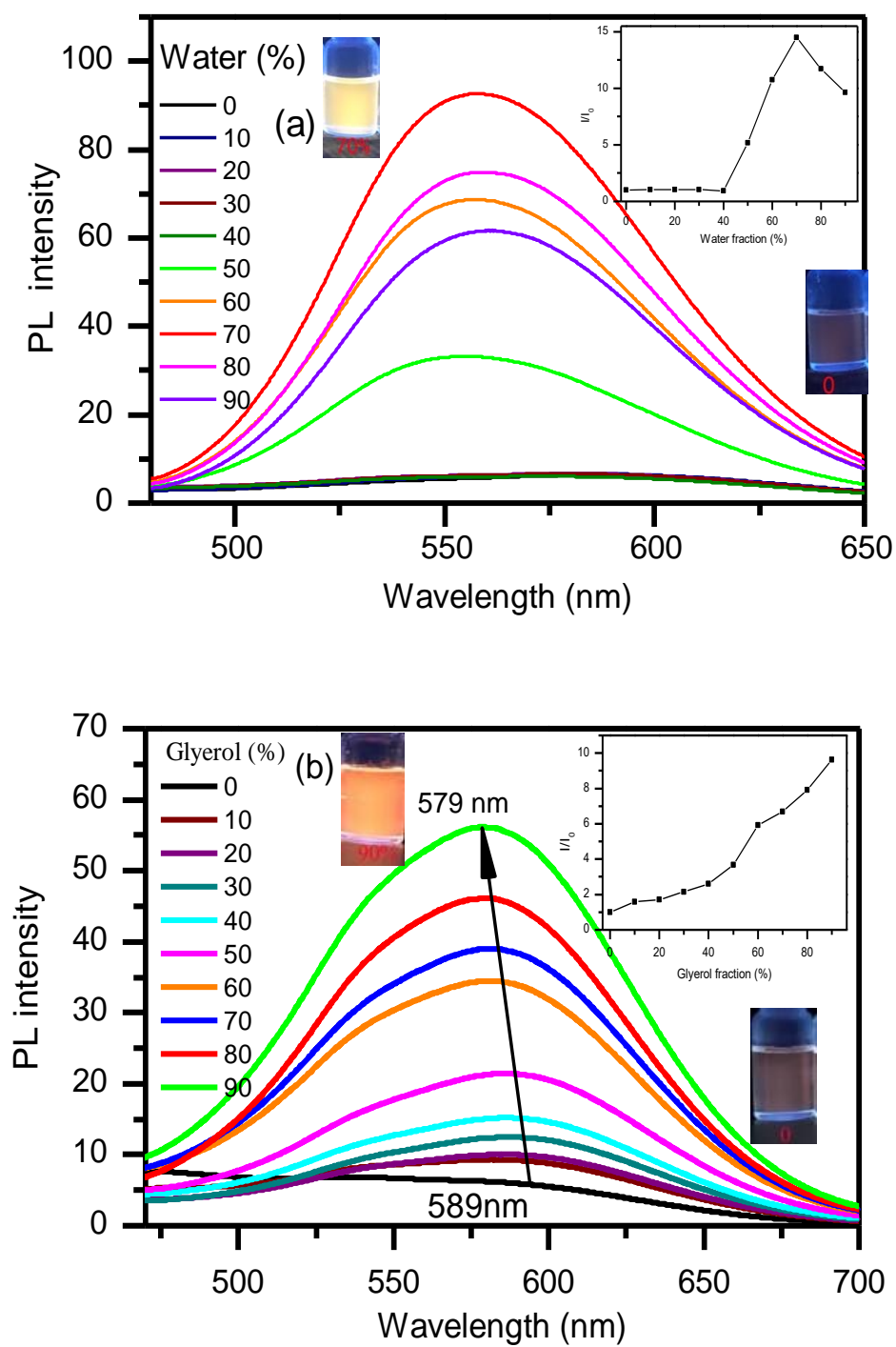


Figure 1 (a) Emission spectra of QUPY (10 μ M) in (a) DMSO/water, (b) THF/water and (c) CH₃CN/water mixtures with different fraction of water. Inset: emission photographs of QUPY (10 μ M) in DMSO and DMSO/water (1/9, v/v). (d) Solid-state emission spectrum of QUPY. inset: photo images of the powder solids for QUPY (λ_{ex} = 365 nm).



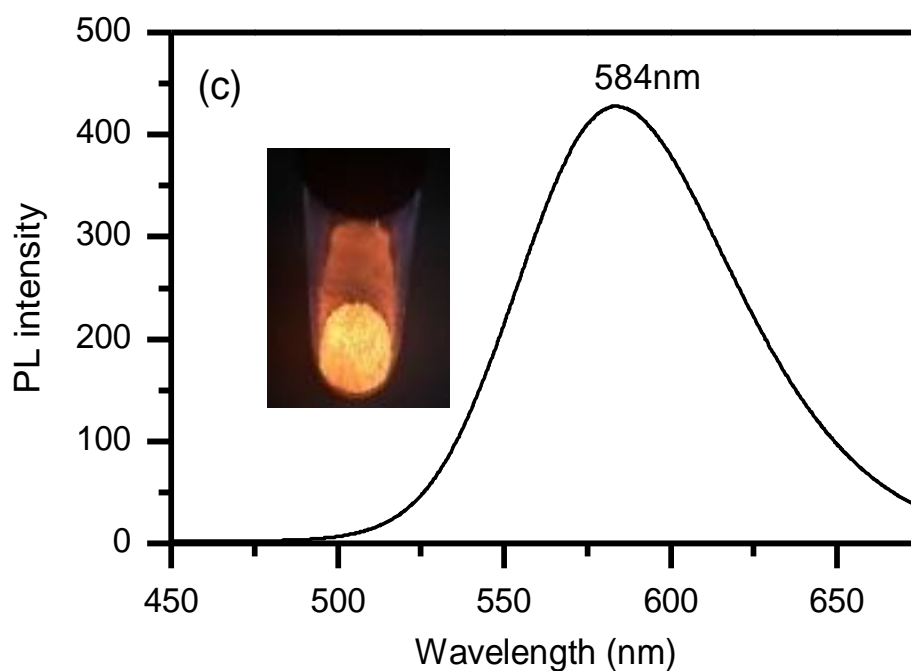


Figure 2 (a) Emission spectra of **QUPY-S** ($10 \mu\text{M}$) in DMSO/water mixtures with different fraction of water. (a) Emission spectra of **QUPY-S** ($10 \mu\text{M}$) in DMSO/glycerol mixtures with different fraction of glycerol. Inset: fluorescence intensity ratio and emission photographs. (c) Solid-state emission spectrum of **QUPY-S**. inset: photo images of the powder solids for **QUPY-S** ($\lambda_{\text{ex}} = 365 \text{ nm}$).

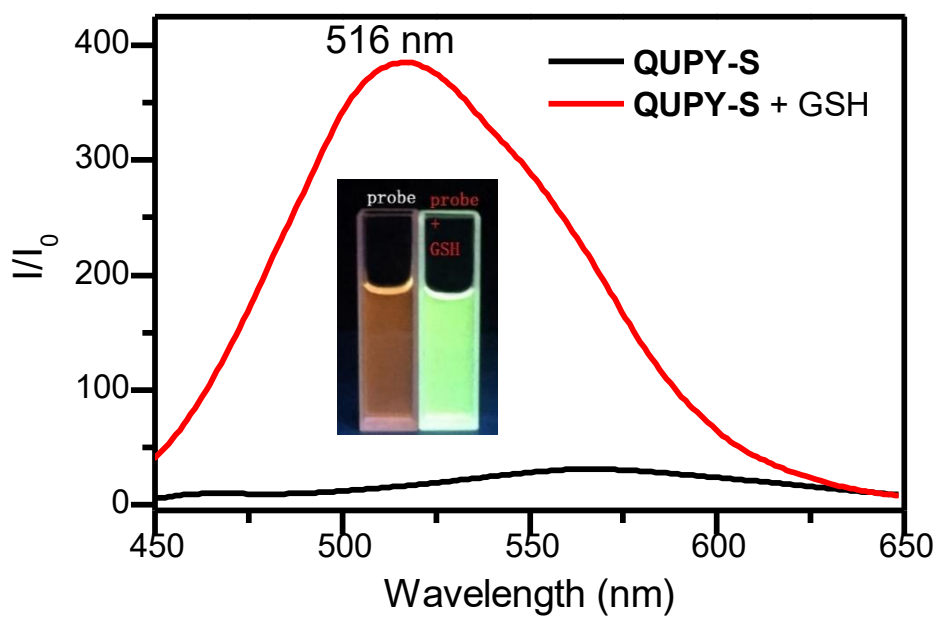


Figure 3 Emission spectra of QUPY-S (10 μM) prior to and after addition of GSH (100 μM) at 37 $^{\circ}\text{C}$ for 90 min in DMSO/PBS ($v/v = 1:1$).

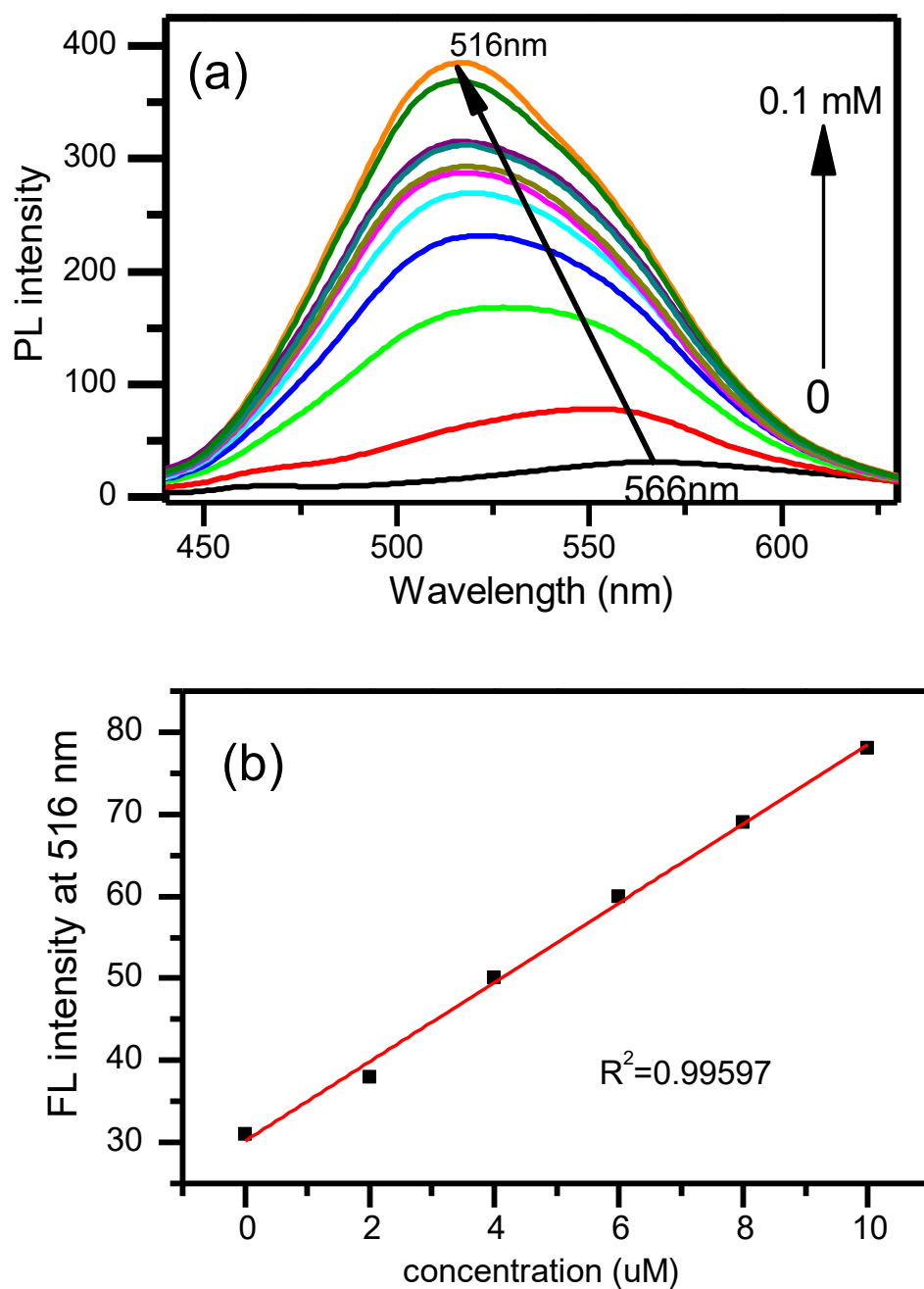


Figure 4 (a) The emission spectra of **QUPY-S** (10 μM) in DMSO/PBS (v/v = 1:1) with increasing GSH (0, 10, 20, 30, 40, 50, 60, 70, 80, 90, 100 μM) at 37 $^\circ\text{C}$ for 90 min. (b) A linear calibration curve between the fluorescent intensity at 516 nm of **QUPY-S** in DMSO/PBS (v/v = 1:1) and the concentration of GSH in the range of 0-10 μM after incubation for 90 min at 37 $^\circ\text{C}$.

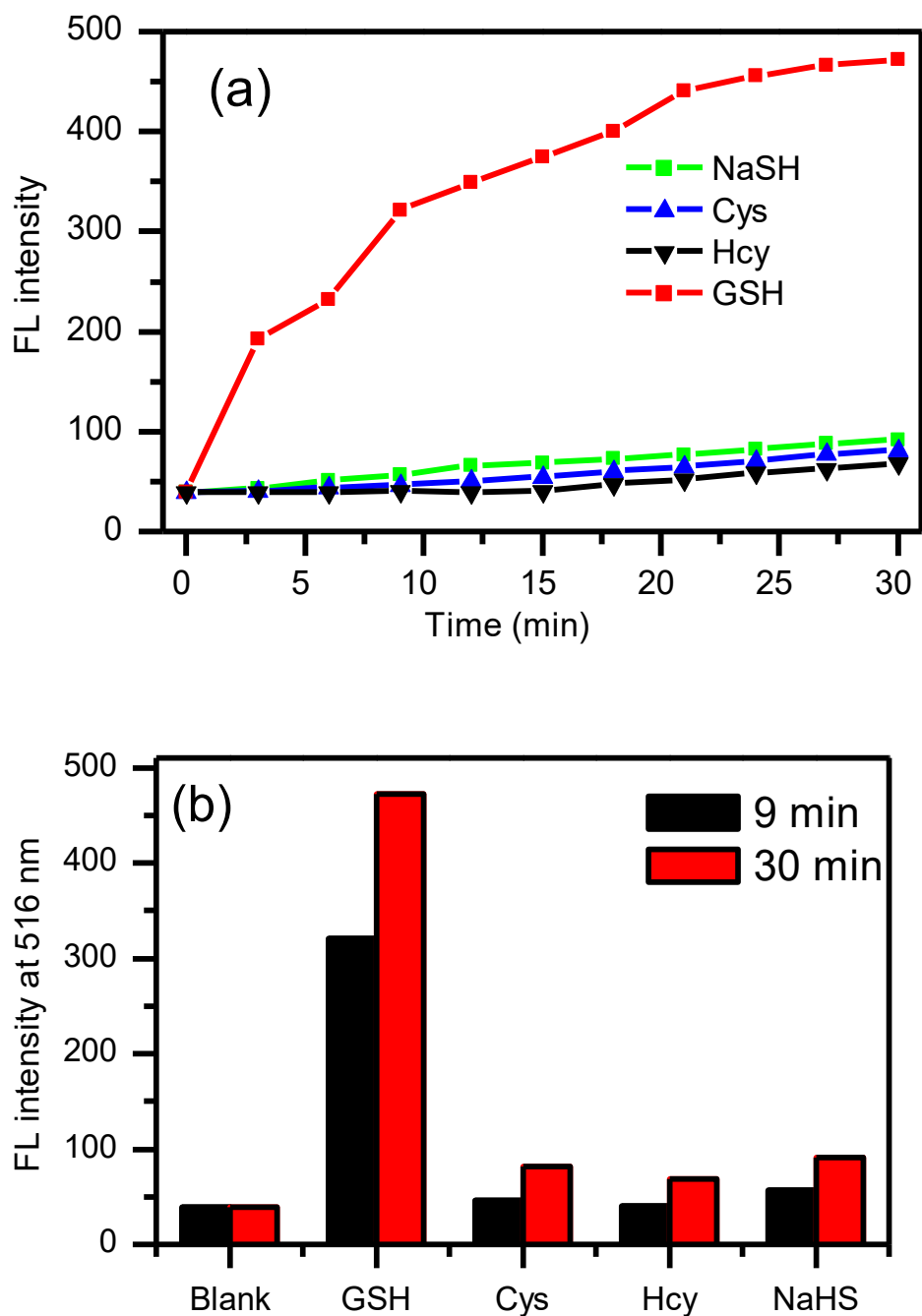


Figure 5 (a) Time-dependent changes of emission spectra of **QUPY-S** (10 μM) in DMSO/PBS buffer (1:1, v/v, pH 7.4) at 37 °C after incubation with GSH (red, 1 mM), Cys (blue, 80 μM), Hcy (black, 80 μM) as mimics of intercellular concentration and NaSH (cyan, 50 μM, typical concentration in blood). (b) Fluorescence intensity of **QUPY-S** (10 μM) in DMSO/PBS buffer (1:1, v/v, pH

7.4) at 37 °C with GSH (red, 1mM), Cys (blue, 80 μ M), Hcy (black, 80 μ M), NaSH (cyan, 50 μ M, typical concentration in blood) as mimics of intercellular concentration and after 9 min (black column) and 30 min (red column).

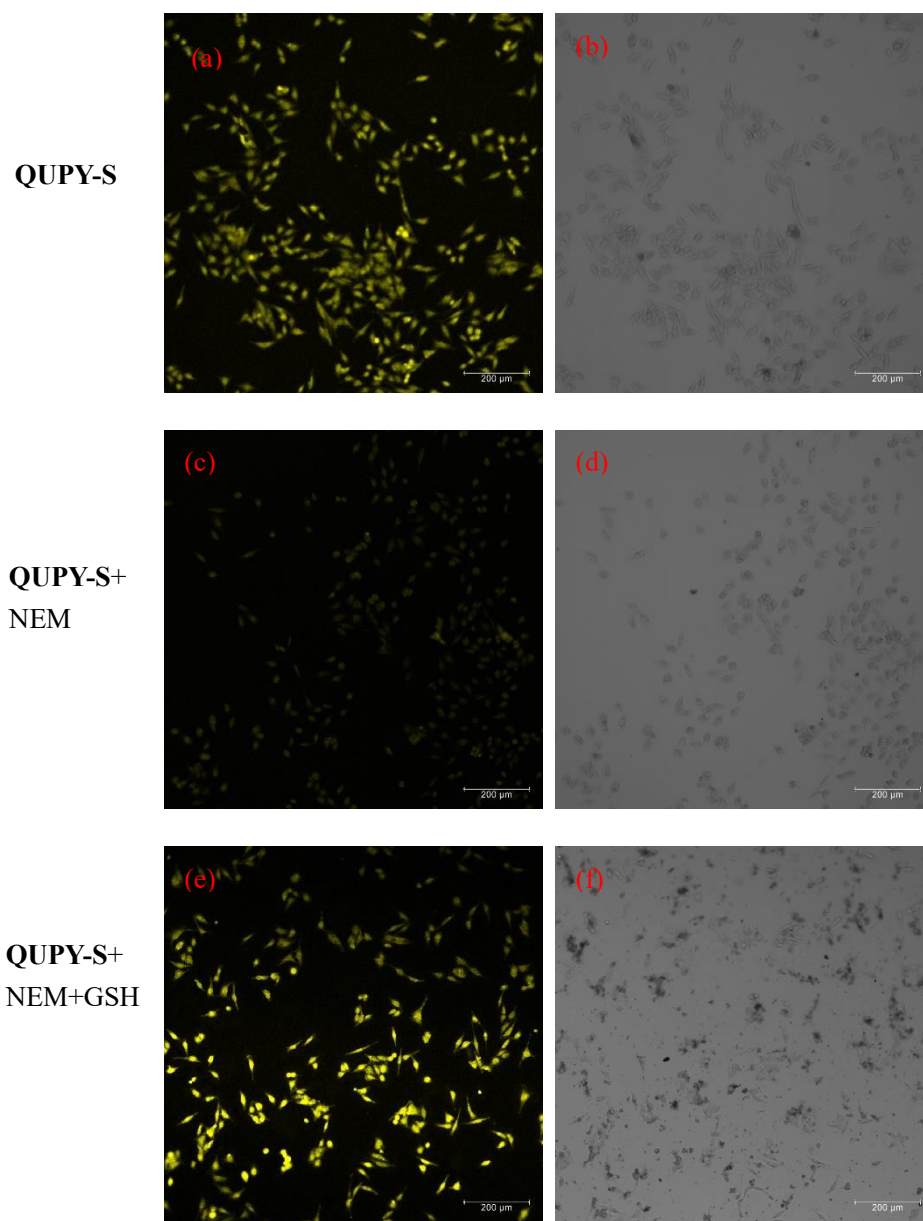


Figure 6 Confocal fluorescence images of HeLa cells. (a) Cells incubated with **QUPY-S** (20 μM) for 30 min; (c) HeLa cells were pre-incubated with 5 mM NEM for 30 min and then treated with **QUPY-S** (20 μM) for 30 min; (e) HeLa cells were pre-incubated with 5 mM NEM for 30 min and then treated with **QUPY-S** (20 μM) and GSH (5 mM) for another 30 min; (b, d and f, phase contrast images; a, c and e, fluorescence images).

Graphic Abstract



A light-up fluorescent probe (**QUPY-S**) for glutathione based on a triphenylethylene-containing quinoxaline pyridinium salt has been developed.